Molecular Biology of the Cell
Vol. 14, 4685–4694, November 2003

Localization and Dynamics of Cdc2-Cyclin B during Meiotic Reinitiation in Starfish Oocytes[V]

Mark Terasaki,*† Ei-ichi Okumura, sup‡ Beth Hinkle,*§ and Takeo Kishimoto‡

*Department of Physiology, University of Connecticut Health Center, Farmington, Connecticut 06032; and ‡Laboratory of Cell and Developmental Biology, Graduate School of Bioscience, Tokyo Institute of Technology, Nagatsuta, Midoriku, Yokohama 226-8501, Japan

Submitted April 21, 2003; Revised July 11, 2003; Accepted July 11, 2003
Monitoring Editor: Mark Solomon

The Cdc2-cyclin B kinase has a central role in regulating the onset of M phase. In starfish oocytes, Cdc2-cyclin B begins to be activated ~10 min after application of maturation hormone, followed by accumulation in the nucleus then nuclear envelope breakdown. By immunofluorescence and by expressing a green fluorescent (GFP) chimera of cyclin B, we find that cyclin B is present in aggregates in the cytoplasm of immature oocytes. The aggregates disperse at ~10 min, suggesting that the dispersal is closely related to the activation of the kinase. Using cyclin B-GFP, the dispersion begins from the region containing the centrosomes. Extractability of Cdc2-cyclin B changes with similar kinetics during maturation. Active Cdc25 phosphatase released Cdc2-cyclin B from the detergent-insoluble fraction independently of its phosphatase activity. Live cell imaging also showed that Cdc2-cyclin B begins to accumulate in the nucleus before changes in nuclear pore permeability, consistent with Cdc2-cyclin B-induced disassembly of the pores.

INTRODUCTION

The Cdc2/*cdk1* kinase triggers the onset of M phase (Nurse, 1990). Activation of Cdc2 requires association with cyclin B and dephosphorylation of Thr 14 and Tyr 15 on Cdc2; the phosphorylation state is governed by the relative activities of Wee1 family kinases and Cdc25 phosphatase (reviewed in Lew and Kornbluth, 1996). Inactive Cdc2-cyclin B is present in the cytoplasm during interphase and after it is activated, accumulates in the nucleus where it phosphorylates multiple targets to cause nuclear envelope breakdown (Pines and Hunter, 1991; Ookata *et al*., 1992).

There are still many aspects of this system that are not well understood. The pathway leading to activation is different in different organisms and has not been established except in starfish (Okumura *et al*., 2002). Phosphorylation of cyclin is probably involved in the regulation of nuclear entry (Li *et al*., 1997; Hagting *et al*., 1998; Toyoshima *et al*., 1998; Yang *et al*., 1998) but may have other roles as well (Peter *et al*., 2002).

Another subject of uncertainty regards Cdc2-cyclin B localization in the cytoplasm and its possible associations with other molecules in the cytoplasm. There are several indications that inactive Cdc2-cyclin B is not free to diffuse in the cytosol but instead, is associated with other molecules or intracellular structures and undergoes changes in associations when it becomes activated. Among various reports, Picard and Peaucellier (1998) observed cyclin B in vesicle-like structures in starfish oocytes, Westendorf *et al.* (1989) found evidence for cyclin B aggregates in immature clam oocytes, and Lee and Kirschner (1996) found evidence for a binding inhibitor of Cdc2-cyclin B that is associated with membranes. More recently, inactive Cdc2-cyclin B was found to be associated with annulate lamellae in immature *Xenopus* oocytes (Beckhelling *et al*., 2003).

Current techniques for localization are subject to limitations of various kinds. The use of green fluorescent protein (GFP) chimeras is promising because localization can be studied in living cells. However, light microscopy has limitations on resolution, and GFP chimeras may be mistargeted due to the presence of the added GFP or to overexpression. With immunofluorescence, molecules can be redistributed, extracted, or can lose their antigenicity depending on what fixative and fixation conditions are used. Associations of Cdc2-cyclin B may be lost or artificially induced when cells are disrupted. In all of these methods, subtler forms of interactions, such as transient associations, may be hard to detect.

Starfish oocytes are well suited for investigations of activation of Cdc2-cyclin B. Immature starfish oocytes are arrested in prophase of meiosis I and are triggered to begin meiotic maturation by the hormone 1-methyladenine (1-MeAde). Nuclear envelope breakdown occurs rapidly (20–30 min after application of hormone) and does not require protein synthesis. 1-MeAde acts on the surface of the oocyte to activate a G_i family G protein, releasing $\beta\gamma$ subunits that are the mediators of the downstream effects (Jaffe *et al*., 1993). Through intermediate steps, Akt/PKB becomes activated, which then phosphorylates and inactivates Myt1 (Okumura *et al*., 2002). This Wee1 family kinase normally keeps Thr 14 and Tyr 15 of Cdc2 phosphorylated. Inactivation of Myt1 is able to relieve the inhibition of Cdc2-cyclin B

Article published online ahead of print. Mol. Biol. Cell 10.1091/mbc.E03–04–0249. Article and publication date are available at www.molbiolcell.org/cgi/doi/10.1091/mbc.E03–04–0249.

[V] Online version of this article contains video materials for several figures. Online version is available at www.molbiolcell.org.

† Corresponding author. E-mail: terasaki@neuron.uchc.edu.

§ Present address: Miravant Medical Technologies, Goleta, CA 93117.

enough to allow positive feed back pathways to activate the rest of the Cdc2-cyclin B pool. Cdc2-cyclin B phosphorylates Cdc25 to activate it, and phosphorylates Myt1 to inactivate it, thus forming a positive feedback loop for Cdc2-cyclin B activation.

In immature starfish oocytes, all of the cyclin B is complexed with Cdc2 (Ookata *et al*., 1992). In these conditions, immunofluorescence of cyclin B should show the localization of Cdc2-cyclin B, and it was shown that Cdc2-cyclin B accumulates in the nucleus before germinal vesicle breaks down (GVBD) (Ookata *et al*., 1992). However, the regulation of nuclear accumulation of Cdc2-cyclin B is not understood and the localization of inactive Cdc2-cyclin B in frog oocytes (Beckhelling *et al*., 2003) suggests that there may be other features of activation that are unknown. The availability of a GFP chimera of cyclin B (Hagting *et al*., 1998) led us to reexamine the localization and dynamics of Cdc2-cyclin B during maturation of starfish oocytes.

MATERIALS AND METHODS

Oocytes

Starfish were obtained from the Bodega Marine Laboratory (Bodega Bay, CA) (*Asterina miniata*) or in Tokyo Bay (*Asterina pectinifera*). Ovaries were isolated and follicle cells removed from the oocytes by treatment in calcium-free seawater as described in Jaffe *et al*. (1993). To induce maturation, oocytes were exposed to 1 μM 1-MeAde (Sigma-Aldrich, St. Louis, MO) at room temperature (~22°C).

Immunofluorescence and Microscopy

Oocytes were dropped into a scintillation vial containing 10 ml of methanol at −70°C. After 1 h, the vials were removed from the freezer and allowed to stand at room temperature for 30 to 60 min. Most of the methanol was removed and replaced with ~10 ml of Ca-Mg–free phosphate-buffered saline (PBS) with azide and was kept at 4°C. For staining, ~12–24 oocytes were transferred to a well in a 60-well Terasaki plate (catalog no. 163118; Nalge Nunc; Naperville, IL). The fluid was replaced with 10 μl of 1:50 diluted affinity purified rabbit anti-starfish cyclin B (Ookata *et al*., 1992). The plate was attached to a rotary motor for slow mixing for ~1 h. The oocytes were removed and put into a 100-μl drop on Parafilm for second antibody incubation. The second antibody, rhodamine (Rh) conjugated goat anti-rabbit (ICN Pharmaceuticals, Costa Mesa, CA) at 1:50 in 100 μl was added. This was incubated for ~1 h, followed by washes, with a final incubation in wash buffer for 10 min. Oocytes were placed in a drop on a microscope slide with a single double stick spacer and a #0 coverslip. For imaging immunofluorescence, as well as cyclin B-GFP, an MRC 600 confocal microscope (Bio-Rad, Cambridge, MA) with a krypton argon laser was used; it was coupled to an upright Axioskop microscope (Carl Zeiss, Thornwood, NY) with a 40 × 1.3 numerical aperture Plan-Neofluar objective lens.

Cyclin B-GFP and Microinjection

Cyclin B-GFP was made with GFP at the C-terminal end as described in Hagting *et al.* (1998). The cyclin B sequence was from *A. pectinifera* (Tachibana *et al*., 1990). The linker sequence was AGAQFLE and the S65T variant of GFP without the start methionine was used (Heim *et al*., 1995). This was cloned into the plasmid SP64-S (Tang *et al*., 1995) with the *A. pectinifera* cyclin B kozak sequence tacaat. mRNA was made with mMessage mMachine (Ambion, Austin, TX) and resuspended in nuclease free water at a concentration of ~1 μg/μl.

Quantitative microinjection was done with mercury loaded pipets as described previously (Hiramoto, 1962; Kiehart, 1982; for more details on procedures and equipment, see http://egg.uchc.edu/injection). For double labeling, 70-kDa rhodamine dextran (Molecular Probes, Eugene, OR) dissolved at 5 mg/ml in injection buffer (100 mM potassium glutamate, 10 mM HEPES, pH 7) was injected to a final concentration of ~20 μg/ml.

Roscovitine was obtained from Sigma-Aldrich and dissolved as a stock solution in dimethyl sulfoxide at 10 mM.

Electrophoresis and Immunoblots

SDS-PAGE was carried out by the method of Laemmli (1970) with 8% acrylamide gels. Immunoblots was performed essentially as described previously (Ookata *et al*., 1992). The primary antibodies for immunoblots were purified rabbit polyclonal antibodies against starfish Cdc25, cyclin B, Myt1 antibodies, and monoclonal antibodies against Cdc2-PSTAIR regions as described previously (Okumura *et al*., 2002). Secondary antibodies for immunoblots were alkaline-phosphatase conjugated anti-rabbit or anti-mouse IgG (Dakopatts, Glostrup, Denmark).

Biochemical Subcellular Fractionation of Maturing Oocytes

For experiment A in Figure 5, oocytes were packed by centrifugation at 3000 × *g* and then 10 volumes of low-salt buffer (20 mM HEPES pH 7.3) were added and mixed using a vortex mixer three times for 10 s at room temperature. The mixtures were centrifuged at 10,000 × *g* for 20 min at 4°C and the supernatant was collected as "soluble" fraction. The low-salt insoluble pellet was resuspended by 1× volume of detergent-containing buffer (20 mM HEPES pH 7.3, 0.5% NP-40) and the supernatant of 10,000 × *g* centrifugation was collected as "detergent-soluble" fraction. The detergent-insoluble pellet was resuspended with the same volume of detergent containing buffer as the "detergent-insoluble" fraction. To prepare for SDS-PAGE, supernatants and suspensions were mixed 1:1 with 2 volumes of Laemmli's sample buffer to make each fraction originate from the same amount of packed oocytes. For experiment B, packed oocytes prepared as mentioned above were mixed with 30 volumes of methanol at −70°C for 1 h and then spun down gently to prevent lysis. Methanol-soluble supernatants were collected and centrifuge evaporated. Methanol-treated oocytes were incubated for 1 h at 4°C with 30 volumes of PBS containing sodium azide and then spun down again. The PBS-soluble fractions were collected and centrifuge evaporated. The evaporated methanol-soluble fraction, PBS solubilized fraction and MeOH/PBS-insoluble fractions were resuspended in the same volume of PBS and then all fractions were mixed 1:1 with Laemmli's sample buffer to make each fraction originate from same amount of packed oocytes.

Release of Cdc2-Cyclin B Complexes by Cdc25 Phosphatase from the Detergent-treated Oocytes

Active and inactive forms of Cdc25 phosphatase were prepared as described previously (Okumura *et al*., 1996). Briefly, Cdc25 proteins were eluted from an anti-Cdc25 immuno-affinity column with 4.5 M $MgCl_2$ and were desalted with a PD-10 column (Pharmacia LKB, Piscataway, NJ) equilibrated with a buffer containing 150 mM NaCl, 50 mM Tris (pH 7.5), 1 mM dithiothreitol and 0.1% NP-40. Cdc25 proteins were concentrated with Ultrafree MC-30 (Millipore, Bedford, MA) at a concentration of 50 μg/ml. Excess volume of 0.5% (wt/vol) NP-40 containing extraction buffer (20 mM PIPES pH 6.8, 5 mM EGTA, 1 mM $MgSO_4$, 20 mM β-glycerophosphate, 1 mM phenylmethylsulfonyl fluoride, 1 mM dithiothreitol) was added to immature oocytes and incubated for 10 min at 4°C with gentle mixing and spun down gently. Precipitated oocytes were further washed with detergent containing buffer several times. The detergent treated oocytes were mixed 1:1 with purified Cdc25 proteins for 1 h at room temperature. Mixtures were centrifuged at 10,000 × *g* for 20 min and supernatants were collected. Precipitates were washed once with Tris-buffered saline and repelleted.

Simultaneous Imaging of Cyclin B-GFP and 70-kDa Rh Dextran

A 20× Plan-Neofluar (0.5 numerical aperture; Carl Zeiss) objective lens was used. The double labeling filters (K1, K2 blocks) were used with a replacement dual excitation barrier filter (Chroma Technology, Brattleboro, VT). For the experiment shown in Figure 7, the laser was at full power and attenuated with a 10% neutral density filter. By using a laser power meter (model 1815-C; Newport, Irvine, CA), there was 160 μW of 488-nm light exiting the 20× objective lens and delivered to the sample. The most relevant value for photodynamic damage is energy delivered per area, because the same amount of energy deposited in a smaller area will cause greater damage. For the zoom 1 setting used for the experiment, the energy density of 488-nm light was 1.6 nW/μm^2. Images in the time-lapse sequence were obtained by a single 1-s scan, which corresponds to 1.6 nJ/μm^2 delivered at the time-lapse interval of 15 s. On the detection side, the confocal aperture was wide open and the gain settings were 850 for the GFP channel and 750 for the Rh dextran channel.

Quantitation of Fluorescence

Calcein (Molecular Probes) was used for calibrating fluorescence levels. Calcein, which is a fluorescein analog with two negative charges, was made as a stock concentration of 0.5 mg/ml in injection buffer, and was injected to 1% volume. It was imaged with identical settings as used for the cyclin B-GFP–expressing oocytes except with a lower transmission neutral density filter. Because the brightness of the cytoplasmic fluorescence depends on the focus level of the objective lens, z series images were taken of oocytes that were either uninjected (for autofluorescence), expressing cyclin B-GFP, or injected with calcein. The z series were taken at 2.0-μm intervals with a low numerical aperture objective lens (10×, 0.3 numerical aperture Plan-Neofluar; Carl Zeiss). There was a relatively broad maximum, so it was straightforward to assign a fluorescence level with this data. To convert calcein and GFP fluo-

rescence differences to concentration differences, we used the relationship that fluorescein is approximately twice as bright as S65T GFP (Terasaki *et al*., 1996).

RESULTS

Cyclin B Is Present in Aggregates in Immature Oocytes and Disperses during Maturation

Immature starfish oocytes are arrested at meiosis I prophase with a large intact nucleus called the germinal vesicle (GV). The maturation hormone 1-MeAde restarts meiosis, during which the germinal vesicle breaks down (GVBD). Oocytes from the same animal undergo GVBD within a few minutes of each other, but there is variation between different animals so that GVBD normally occurs between ~15 and 30 min after application of 1-MeAde.

To localize Cdc2-cyclin B by immunofluorescence, we used an antibody to cyclin B similar to that used previously (Ookata *et al*., 1992). On a Western blot, the rabbit antibody to starfish cyclin B stained a single band of the expected molecular weight. Imaging by confocal microscopy of whole, methanol fixed, immature oocytes showed spots in the cytoplasm as well as staining of the nuclear envelope (Figure 1). The spots were not seen in formaldehyde-fixed cells. The spots had a diameter of ~1 μm. The number and distribution of spots varied somewhat in oocytes from different animals; in a z series sequence of a representative oocyte, there were ~2000 spots. When the Golgi apparatus was localized by galtransferase-GFP expression, it also shows as spots scattered throughout the cytoplasm (Terasaki, 2000), but double staining by cyclin B immunofluorescence showed that the Golgi apparatus and spots were not colocalized (our unpublished data). Cyclin B is not associated with annulate lamellae as in *Xenopus* oocytes (Beckhelling *et al*., 2003) because starfish oocytes do not possess annulate lamellae by electron microscopy or by immunofluorescence labeling (our unpublished data).

The spots disappeared during maturation (Figure 2). In the sequence shown, the spots were unchanged at 5 min, noticeably less at 10 min, were clearly disappearing at 15 min, and had completely disappeared at 20 min. The spots in the center of the oocyte seemed to disappear last. GVBD occurred at ~25 min in oocytes from the animal used for this time series. The timing of disappearance is of particular interest because it is similar to the appearance of H1 kinase activity (Ookata *et al*., 1992). The disappearance of the spots is probably closely related to the activation of the Cdc2 kinase.

Cyclin B GFP Localizes to Aggregates

A functional GFP chimera of human cyclin B had been reported in which GFP is attached at the C terminal (Hagting *et al*., 1998). We made a similar construct using the previously cloned cyclin B from the starfish *A. pectinifera* (Tachibana *et al*., 1990). mRNA coding for this construct was injected into immature starfish oocytes (*A. miniata*). After overnight incubation, there was fluorescence in the cytoplasm but not the GV (Figure 3), as expected for cyclin B (Ookata *et al*., 1992). A similar distribution was seen when mRNA coding for the human cyclin B-GFP was injected.

The expression level of cyclin B-GFP affected the timing of GVBD. At moderate levels, GVBD occurred 5–10 min earlier than in uninjected controls, whereas at high levels, GVBD was even earlier or occurred spontaneously. The concentration of endogenous cyclin B in starfish oocytes is estimated to be 20 nM (Tachibana and Kishimoto, unpublished data), which corresponds to 12 molecules/μm^3 if the cyclin B is uniformly distributed. This seems near the detection limit of the confocal microscope, though if most of the cyclin B is present in aggregates, it may be easier to image the aggregates. In the experiments shown here, the amount of cyclin B-GFP was ~10× greater than endogenous 20 nM (see MATERIALS AND METHODS and section on accumulation in the nucleus). This resulted in a speed up of the timing of GVBD by 5–10 min, but it allowed easier imaging and gave similar results as with lower expression levels.

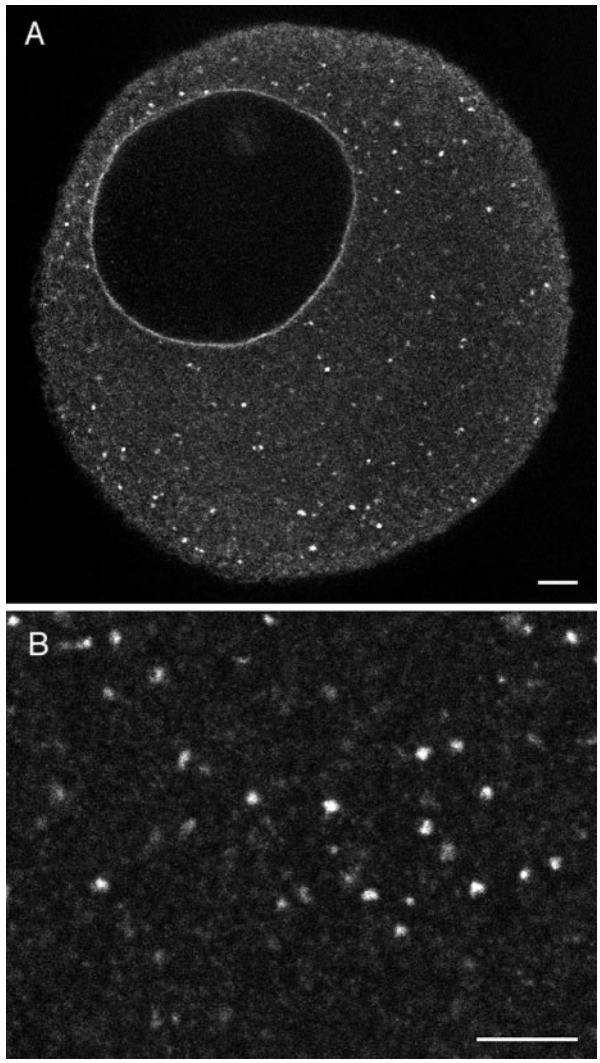

Figure 1. Immunofluorescence labeling of cyclin B in immature starfish oocytes. (A) Small spots are seen scattered through the cytoplasm, and the nuclear envelope is also stained. (B) Higher magnification view. Bar, 10 μm.

When cyclin B-GFP was imaged by confocal microscopy, small spots were seen, corresponding well with immunofluorescence (Figure 3). This correspondence of cyclin B-GFP localization in living cells with immunofluorescence localization in methanol-fixed cells, but not formaldehyde-fixed cells, is similar to that seen in *Drosophila* (Huang and Raff, 1999). The cyclin B-GFP spots disappeared during maturation with kinetics similar to those seen with immunofluorescence. In addition, there was a spatial pattern to the disappearance. The GV is located within 5–10 μm of the cell surface at the animal pole (the site of polar body extrusion),

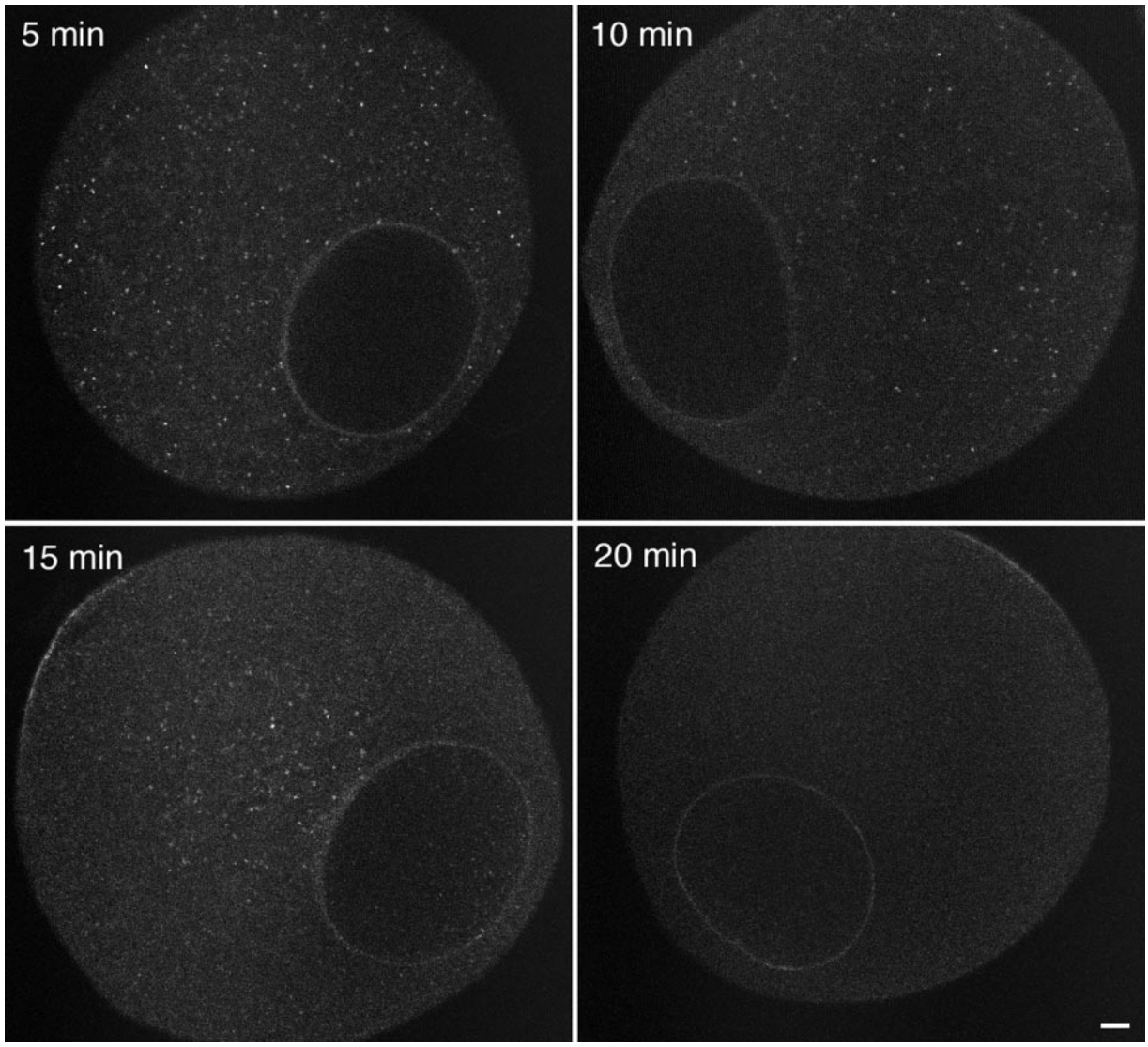

Figure 2. Cyclin B localization during maturation. Oocytes were exposed to the maturation hormone 1-MeAde then fixed at 5-min intervals for immunofluorescence, as indicated on the figure. By 20 min, all of the spots are gone; spots in the middle of the oocyte seem to be last to disappear. Most of the oocytes had undergone GVBD by 25 min. These are representative images, but there was a significant amount of variation. "immfl.mov" is a movie file containing all of the stained oocytes at each time point in this experiment. Bar, 10 μm.

and the centrosomes are present in this small space between the GV and cell surface (Otto and Schroeder, 1984). When the oocyte was imaged in an orientation so that the animal-vegetal axis was in the plane of focus, it was possible to see the timing of the disappearance of these spots relative to the oocyte polarity. The spots disappeared from the animal pole side first, spreading around the cortex (Figure 3), with the spots in the center of the oocyte disappearing last. The timing of the wave is ~3 min; if this is calculated according to the circumference of the egg, the speed is 3 μm/s.

The cyclin B-GFP spots were photobleached to characterize the dynamics within the spots. After photobleaching, the image of the same spot reappeared and became as bright as the original (Figure 4). The half-time for recovery was 20.1 s (SD = 1.2; N = 7, from four oocytes). This indicates that there is relatively rapid turnover of Cdc2-cyclin B within the spot.

We tested whether an inhibitor of *cdc2* kinase activity would affect the aggregates or their dispersal. Roscovitine is a purine analog that is an inhibitor of purified *cdc2*-cyclin B (IC_{50} = 0.65 μM) and blocks 1-MeAde–induced maturation at somewhat higher concentration (IC_{50} = 5 μM) (Meijer *et al*., 1997). In the absence of 1-MeAde, roscovitine (20 μM) unexpectedly caused the disappearance of the cyclin B-GFP spots by ~10 min. Because *cdc2* kinase activity is already low in immature oocytes, this effect is probably not due to simply inhibiting the kinase activity. Instead, roscovitine might bind to a site involved in cdc2-cyclin B association with the aggregates or might cause a conformational change in cdc2-cyclin B, which prevents association.

Cyclin B Extractability Changes during Maturation

The cyclin B immunofluorescence and cyclin B-GFP imaging indicates that a significant amount of Cdc2-cyclin B is not

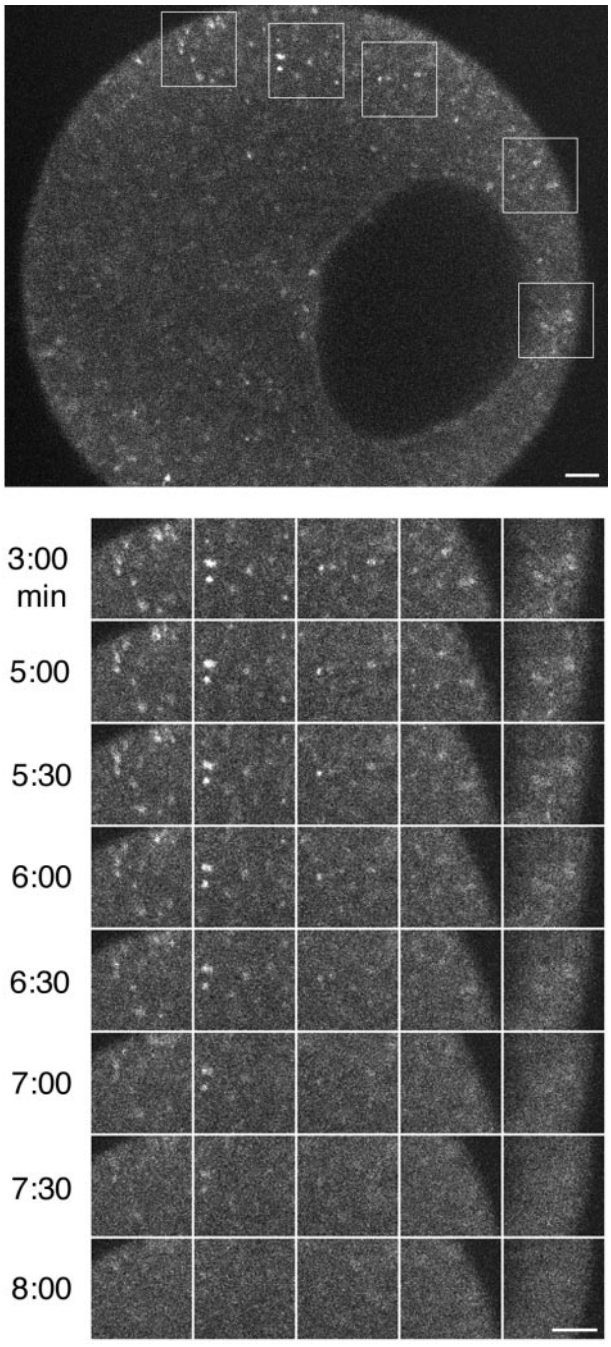

Figure 3. Cyclin B-GFP time course during maturation. Cyclin B-GFP was expressed by injection of mRNA. Spots in immature oocyte correspond to spots seen by immunofluorescence. In time-lapse sequences of an oocyte during maturation, the spots disappeared beginning near the animal pole. "cb.mov" is a movie of this sequence, including cyclin B entry into the nucleus. To document the sequence of disappearance, five areas were selected (white rectangles on the full image) and are shown below, with the time elapsed after addition of the maturation hormone 1-MeAde sequence is shown at the left. The nucleus broke down at 15 min. Bar, 10 μm.

freely diffusing in immature oocytes. To further characterize Cdc2-cyclin B associations with cytoplasmic components during maturation, immature and maturing oocytes at several time points after 1-MeAde addition were extracted with low-salt buffer and then with detergent-containing buffer. Thus, three fractions were separated: (A1) soluble (soluble in treatment with low-salt buffer), (A2) detergent soluble (insoluble after low-salt buffer treatment, but soluble in the detergent-containing buffer), and (A3) detergent insoluble (insoluble after treatment with detergent-containing buffer). In these fractions, Cdc25, cyclin B, Cdc2, and Myt1 proteins were monitored by immunoblotting (Figure 5A). Cyclin B was present in all three fractions from immature and maturing oocytes. In immature oocytes the amount in each fraction was ~25% in A1, 50% in A2, and 25% in A3. Myt1 was detectable only in A2, and Cdc25 (our unpublished data) only in A1. After 1-MeAde addition, the amount of cyclin B in A1 increased by ~10–15% of the total cyclin B, supporting the release of cyclin B from either A2 or A3, or both. In addition the immunoblotting data show that Cdc2-cyclin B begins to be activated soon after 1-MeAde addition and is fully activated soon after GVBD (Ookata *et al.*, 1992). A large amount of cyclin B remained in the detergent-soluble and -insoluble fractions (A2 and A3) in maturing oocytes. Some may be associated with the nuclear envelope, which is labeled by immunofluorescence and by cyclin B-GFP (Figures 2 and 3) or may be associated with other structures such as intermediate filaments.

A second extraction scheme was used that corresponds closely to the conditions used for immunofluorescence. Oocytes were extracted first by methanol at −70°C and then, by Ca-Mg–free PBS. Thus, three fractions were separated: (B1) "methanol soluble", (B2) "PBS soluble", and (B3) "MeOH/PBS insoluble." Myt1 and cyclin B were not detectable in B1 (Figure 5B). Myt1 was detectable in B3, whereas cyclin B was detectable in both B2 and B3 with a ratio of ~25% in B2 and 75% in B3. There was little change in this ratio during maturation, when Cdc2-cyclin B is becoming activated; this indicates that methanol does not differentially affect inactive and active Cdc2-cyclin B.

Experiments were done to see whether the detergent-insoluble inactive Cdc2-cyclin B could be solubilized in vitro. The detergent-insoluble fraction was treated with the inactive or active form of Cdc25 phosphatase (Okumura *et al.*, 1996) for 1 h and then separated into soluble and insoluble fractions that were monitored for Cdc2 by Western blots. The active form, but not the inactive form, of Cdc25 caused solubilization of Cdc2 (Figure 6). Vanadate, which is an inhibitor of the tyrosine phosphatase activity of Cdc25, had no effect (Figure 6), showing that the solubilization is independent of the phosphatase activity of Cdc25, but dependent on the active form, of Cdc25.

Imaging of Cyclin B Accumulation in the Nucleus

Immunofluorescence showed that cyclin B accumulates in the nucleus before GVBD, and the images seemed to show that the cyclin B enters first from the animal pole side (Ookata *et al.*, 1992). In time-lapse sequences taken during maturation, cyclin B-GFP similarly accumulates in the nucleus before GVBD. To demonstrate this clearly, cyclin B-GFP was imaged simultaneously with 70-kDa Rh dextran injected into the cytosol. We previously found two phases of 70-kDa dextran entry during maturation, a slow uniform increase throughout the GV beginning around 5 min before GVBD, and then a massive entry from one or two points at the time of GVBD corresponding to a disruption of the membrane permeability barrier of the nuclear envelope (Terasaki, 1994; Terasaki *et al.*, 2001).

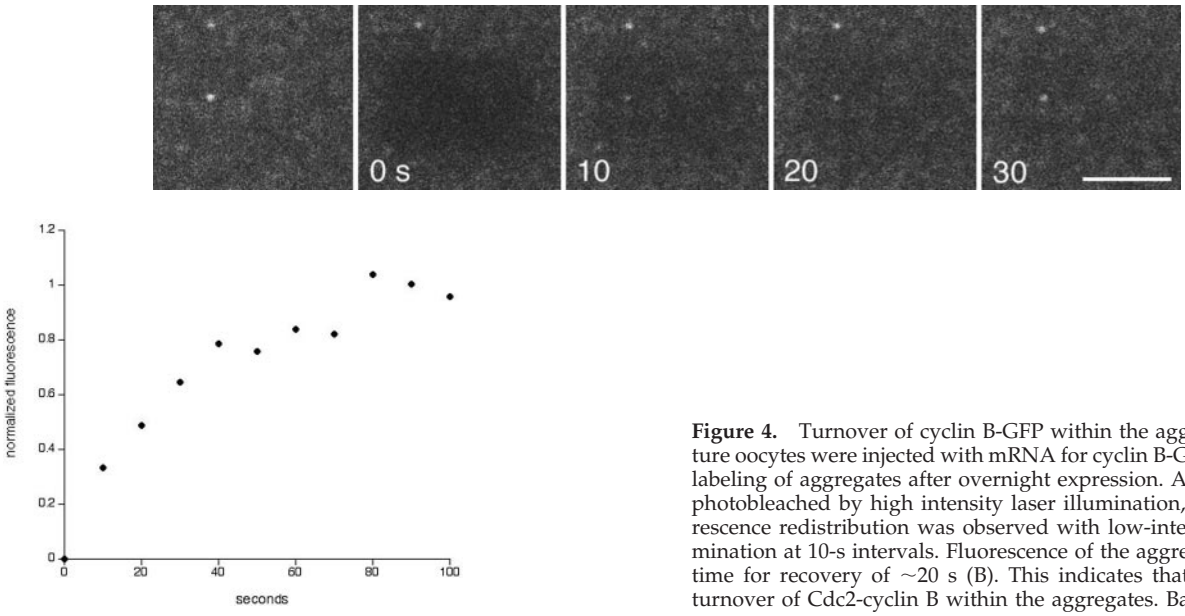

Figure 4. Turnover of cyclin B-GFP within the aggregates. Immature oocytes were injected with mRNA for cyclin B-GFP, resulting in labeling of aggregates after overnight expression. Aggregates were photobleached by high intensity laser illumination, and then fluorescence redistribution was observed with low-intensity laser illumination at 10-s intervals. Fluorescence of the aggregate had a half time for recovery of ~20 s (B). This indicates that there is rapid turnover of Cdc2-cyclin B within the aggregates. Bar, 10 μm.

The fluorescence of cyclin B-GFP and 70-kDa Rh dextran was monitored within a rectangular region in the center of the GV. Data from two oocytes are shown (Figure 7, A and B); the oocytes were estimated to have 210 and 160 nM cyclin B-GFP, respectively (compared with the estimated 20 nM endogenous cyclin B). The oocytes underwent GVBD at 16.8 and 20.4 min after addition of 1-MeAde. Uninjected oocytes from the same batch and incubated identically as the injected oocytes, underwent GVBD at 23.4 min (SD = 2.8; N = 19). After a lag period, cyclin B-GFP in the GV began to increase (Figure 7A) followed by accumulation at a constant rate until a minute or two before GVBD (Figure 7, A and B). Several minutes after cyclin B-GFP began to enter the GV, the 70-kDa dextran began to enter. If the timing is normalized to the time of GVBD, cyclin B-GFP began to enter a little after 0.5, whereas 70-kDa dextran began to enter at ~0.75. Data from a third oocyte in this experiment was similar to that of the first oocyte described. In several other experiments where we either did not estimate the amount of expressed cyclin B-GFP or did not compare the timing of GVBD with respect to that of uninjected controls, cyclin B-GFP and 70-kDa Rh dextran always entered the nucleus with a similar relationship in time.

From time-lapse sequences, it seemed that cyclin B-GFP entered initially from the animal pole side (Figure 7C). This may be a consequence of the apparent initiation of Cdc2-cyclin B activation in the animal pole region (Figure 3).

DISCUSSION

We used three different methods to localize Cdc2-cyclin B in starfish oocytes. By immunofluorescence and expression of a GFP chimera, Cdc2-cyclin B is present in aggregates in immature oocytes that become dispersed during maturation. In salt- and detergent-extracted oocytes, some of the Cdc2-cyclin B moves to the low-salt soluble fraction during maturation. The timing of these changes in localization and extractability corresponds very well with the timing of Cdc2-cyclin B activation as assayed by H1 kinase activity (Ookata *et al*., 1992).

There are uncertainties regarding the results from each of the three methods. The aggregates are seen by immunofluorescence in methanol fixed oocytes, but they are not seen with formaldehyde fixation. Live cell imaging with cyclin B-GFP chimera is problematic because the endogenous concentration of cyclin B is relatively low. Also, the observed fast turnover in the aggregates could mean that it is difficult to preserve the aggregates during extractions. The agreement of the three methods provides strong evidence that a significant fraction of the inactive Cdc2-cyclin B is not freely soluble in the cytoplasm and that at least some of this fraction is released at the activation. Our results are similar to those of Westendorf *et al.* (1989) who described cyclin B aggregates in clam oocytes that disperse on oocyte activation, and to Beckhelling *et al.* (2003) who found an association of Cdc2-cyclin B with annulate lamellae in frog oocytes that disperses during oocyte maturation.

There are several important unresolved issues. The composition of the aggregates in starfish oocytes is not known. It is possible that the aggregates consist solely of Cdc2-cyclin B. In neurons, for instance, calcium/calmodulin-dependent kinase II seems to self-aggregate under certain conditions (Tao-Cheng *et al*., 2002). Other possibilities are that Cdc2-cyclin B binds to a scaffold-like protein, or that Cdc2-cyclin B is cross-linked by binding to other cell cycle regulatory molecules. A related issue is whether the aggregates are associated with membranous or cytoskeletal structures.

Another uncertainty concerns the fraction of total Cdc2-cyclin B that is soluble, in the aggregates, or associated with the nuclear envelope. It is very possible that Cdc2-cyclin B has other associations as well. Light microscopy can only detect relatively large structures, so that associations with small structures may be missed. Also, some types of associations will not be preserved during fixation or during cell extractions.

The nature of the process of aggregate dispersal is unknown as well. One possibility is that activation occurs within the aggregates and that this causes the dispersal. Another possibility is that Cdc2-cyclin B becomes acti-

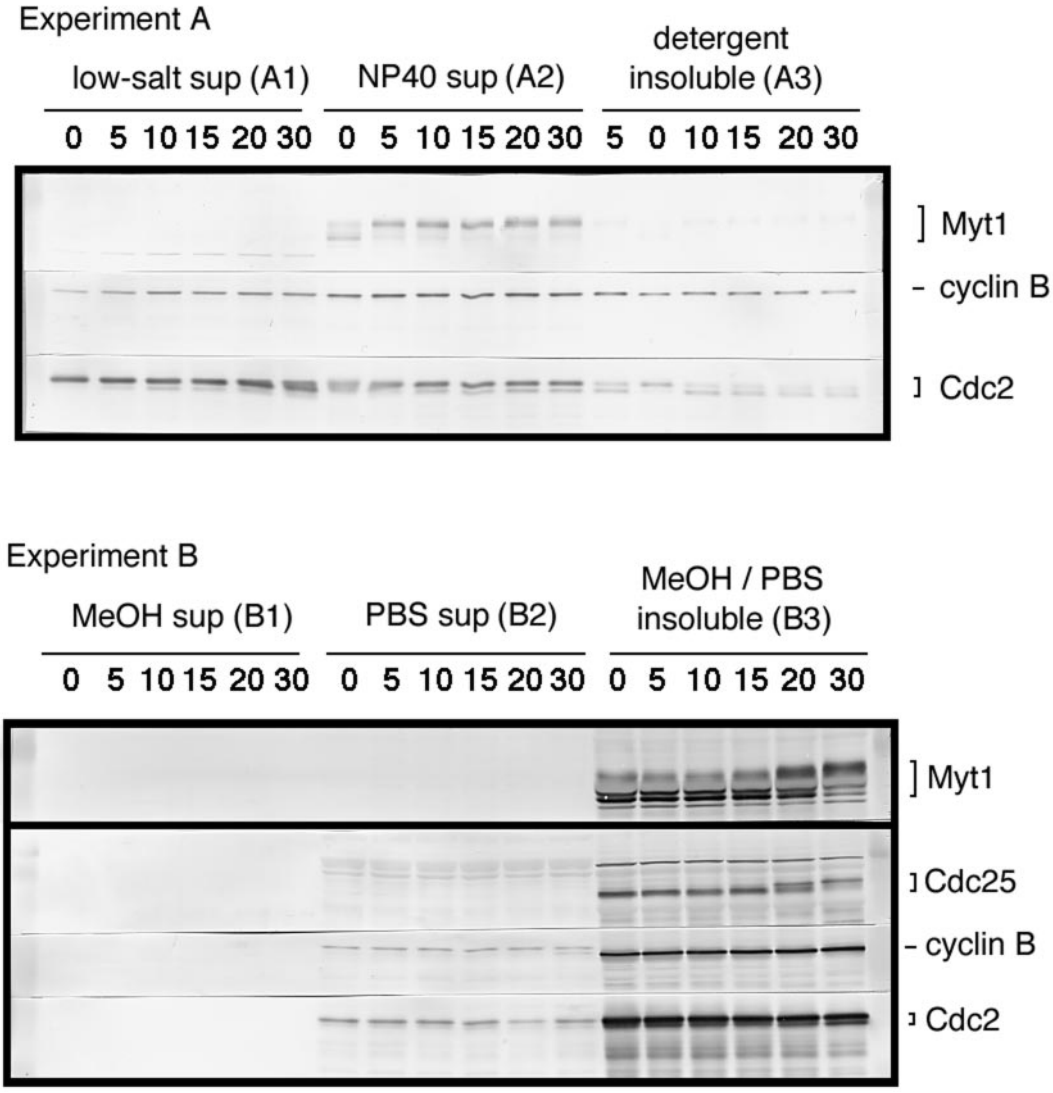

Figure 5. Biochemical subcellular fractionation of Cdc25, cyclin B, Cdc2, and Myt1. Cellular extracts of maturing oocytes were subjected to biochemical fractionation and then analyzed by immunoblots as described in MATERIALS AND METHODS. (A) Soluble, detergent-soluble, and detergent-insoluble fractions prepared from the same amount of maturing oocytes after hormone treatment. (B) Methanol-soluble, PBS-soluble, and PBS-insoluble fractions were prepared in conditions closely corresponding to that used for immnofluorescence.

vated while it is soluble and that dispersal is a downstream effect.

Biochemical fractionation experiments may provide answers to some of these issues. Ten to 15% of the total Cdc2-cyclin B becomes extractable by low salt during maturation (Figure 5, experiment A). One possibility is that this represents the fraction of Cdc2-cyclin B that is in the aggregates. The active form of Cdc25 solubilizes Cdc2-cyclin B in vitro. The phosphatase activity of Cdc25 is not required, so this might occur through a direct and specific association of Cdc25 and Cdc2 (Jessus and Beach, 1992; Zheng and Ruderman, 1993). Initial activation of Cdc2-cyclin B could activate a small amount Cdc25, which would release Cdc2-cyclin B from aggregates as well as activate it, forming a positive feedback loop. One difficulty is that the extraction experiments indicate that in vivo, more than half of total Cdc2-cyclin B is associated with the low-salt unextractable fractions even after GVBD, whereas the in vitro experiments indicate that most of the Cdc2-cyclin B is released from the low-salt unextractable fractions by the active form of Cdc25. One way to explain this is that in vivo, after the release, some part of Cdc2-cyclin B is restored into the low-salt unextractable fractions. That is, the putative restoration system is missing in the in vitro release experiment. The presence of this putative restoration system may be supported by the photobleaching experiments, which indicate relatively rapid turnover of Cdc2-cyclin B in the aggregates (Figure 3).

A modeling approach has also been used (see Slepchenko and Terasaki, in this issue). The turnover within the aggregates indicates that there is a constant association and dissociation of inactive Cdc2-cyclin B. If the association is inhibited, the aggregates could disperse due to continuing dissociation. In the model, Cdc2-cyclin B is activated, whereas in the soluble pool, the resulting depletion of the pool of soluble inactive Cdc2-cyclin B causes the dispersal.

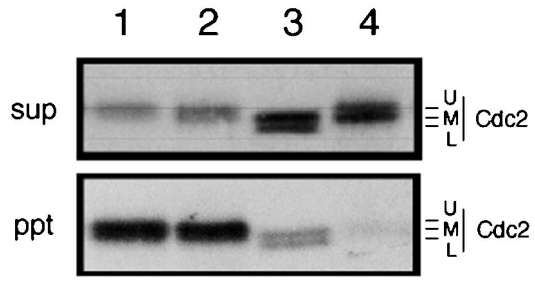

Figure 6. Cdc2-cyclin B complexes were released from detergent-treated oocytes by the active form of Cdc25 phosphatase independently of its phosphatase activity. Detergent-treated oocytes were incubated with buffer (lane 1), the inactive form (lane 2) or the active form of Cdc25 phosphatase in the absence (lane 3) or presence (lane 4) of vanadate for 1 h, and then separated into soluble and insoluble fractions. Cdc2 proteins of each fraction were monitored by immunoblots. U, inactive Cdc2 associated with cyclin B; M, inactive Cdc2; L, active Cdc2 associated with cyclin B.

From an analysis of the activation pathway kinetics, the presence of the aggregates ensures a reliable and complete activation of Cdc2-cyclin B.

Initiation and Propagation of Cdc2-Cyclin B Activation

In time-lapse sequences of the cyclin B-GFP chimera, there was a wave of dispersion that began on the side of the oocyte containing the centrosomes. This is consistent with earlier work in frog eggs, where the initial activation of Cdc2-cyclin B occurs in the animal half and progresses to the vegetal half (Rankin and Kirschner, 1997; Perez-Mongiovi *et al*., 1998); later work showed that centrosomes and nuclei are the most important components of the animal half for Cdc2-cyclin B activation (Beckhelling *et al*., 2000; Perez-Mongiovi *et al*., 2000), and most recently, it was found that an active phosphorylated form of cyclin B occurs first on the centrosomes in cultured mammalian cells (Jackman *et al*., 2003). It seems then that the vicinity of the centrosomes is the decision-making region for entry into M phase, analogous to the initial segment of a neuron where action potentials are initiated.

Accumulation in the Nucleus

It was previously shown by immunofluorescence that cyclin B accumulates in the nucleus before GVBD (Ookata *et al*., 1992). Also in previous work, it was shown that there was a change in nuclear envelope permeability before nuclear envelope breakdown (Terasaki, 1994; Terasaki *et al*., 2001). To observe both of these processes together, cyclin B-GFP entry was imaged by confocal microscopy in parallel with entry of 70-kDa Rh dextran. Entry of 70-kDa dextran indicated that the size cut-off for passive permeability through nuclear pores had increased (Terasaki, 1994). Quantitative studies of dextran entry and time-lapse imaging of a nuclear pore GFP chimera support the idea that nuclear pore disassembly occurs during the period before nuclear envelope breakdown (Terasaki *et al*., 2001; Lénárt *et al*., 2003).

One possibility was that Cdc2-cyclin B, whose molecular weight is ~80 kDa, enters the nucleus passively just as 70-kDa dextran. Instead, cyclin B-GFP began to enter the GV before 70-kDa dextran first began to enter (Figure 7). This shows that Cdc2-cyclin B does not enter due to a change in the passive permeability of the nuclear envelope and is instead consistent with the recent evidence that Cdc2-cyclin B entry is due to changes in active export/import rates (Hagting *et al*., 1998, 1999; Toyoshima *et al*., 1998; Yang *et al*., 1998).

The timing of Cdc2-cyclin B entry is also consistent with a role in causing nuclear pore disassembly. Several nuclear pore components have been shown to become either phosphorylated or hyperphosphorylated during mitosis (Macaulay *et al*., 1995; Favreau *et al*., 1996). The lag between the entry of Cdc2-cyclin B and the first signs of increased passive permeability seems relatively lengthy. Perhaps Cdc2-cyclin B must interact with other proteins before the nuclear pores are affected. Also, several steps of nuclear pore disassembly may have to occur before there is an effect on the passive permeability.

The large size of the starfish nucleus allowed us to observe that cyclin B-GFP initially enters from the animal pole side, which is the location of the centrosomes. This confirms the initial immunofluorescence images of cyclin B accumulation in the starfish nucleus (Ookata *et al*., 1992). It is currently thought that Cdc2-cyclin B accumulates in the nucleus due to phosphorylation, which affects the balance of cyclin B import and export rates between the nucleus and cytoplasm (Hagting *et al*., 1998, 1999; Toyoshima *et al*., 1998; Yang *et al*., 1998). We observed cyclin B staining and cyclin B-GFP localization at the nuclear envelope in immature oocytes, and these may be the molecules that are undergoing nuclear import and export. The location of the initial entry suggests that the first molecules to be phosphorylated are near the centrosomes. In starfish, cyclin B may be phosphorylated by an intermolecular action of Cdc2-cyclin B (Borgne *et al*., 1999). Our observation of entry of cyclin B-GFP suggests that activation of Cdc2-cyclin B first occurs in the region of the centrosomes.

After the cyclin B-GFP had begun to enter the starfish GV, it accumulated in the GV at a linear rate. The constant entry rate is consistent with an active process; it can be contrasted with the passive entry of 10-kDa fluorescent dextran through nuclear pores, which follows an exponential decay because its movement is determined solely by the concentration gradient (Peters, 1984; Terasaki *et al*., 2001). The constant rate of entry of cyclin B-GFP lasted for several minutes. One possible reason for this long period is that the import rate of Cdc2-cyclin B is saturated, leading to a constant, maximal rate of entry; a second possibility is that the cytoplasmic cyclin B is being phosphorylated at a constant rate.

Although many of the key molecules that regulate M-phase initiation seem to have been identified, there is considerable uncertainty regarding how they function together and to what degree movement between cell compartments is crucial (reviewed in Pines, 1999; Takizawa and Morgan, 2000). The experimental advantages of the starfish oocyte, with its rapid meiotic cell cycle and convenience for microscopy and biochemistry (Kishimoto, 1999), should allow it to continue as a useful physiological model system for cell cycle regulation.

ACKNOWLEDGMENTS

We thank Kazunori Tachibana for the starfish cyclin B DNA clone and also Jonathan Pines and Anya Hagting for human cyclin B clone, which was used in preliminary experiments. We thank Laurinda Jaffe, Evelyn Houliston, Ann Cowan, and Kathy Foltz for reading the manuscript. This work was supported by National Institutes of Health grant RO1-GM60389 and by a grant from the Human Frontiers Foundation.

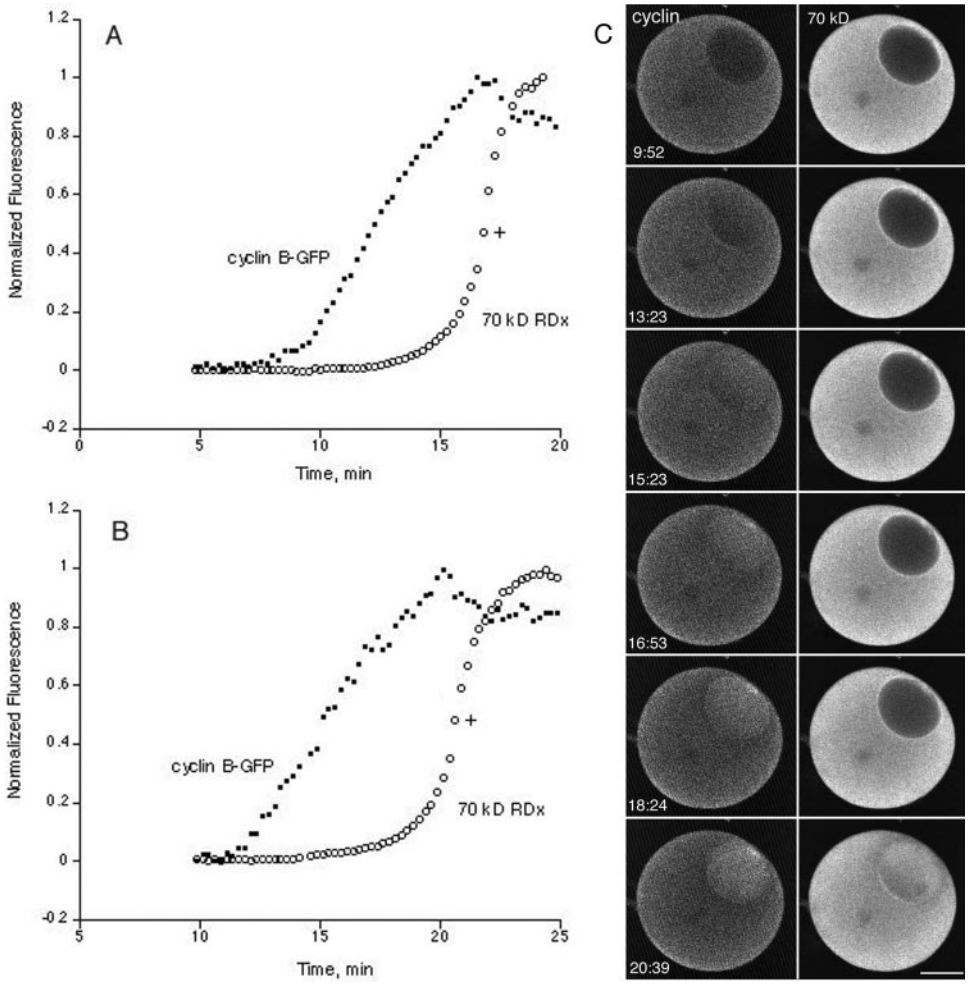

Figure 7. Nuclear entry of cyclin B-GFP and 70-kDa rhodamine dextran during starfish oocyte maturation. Oocytes were injected with mRNA coding for cyclin B-GFP, then after overnight incubation for expression, they were injected with 70-kDa rhodamine dextran (20 μg/ml final concentration) then imaged during 1-methyladenine induced oocyte maturation. (A and B) The fluorescence was measured in a 14 $\times$ 22-μm (30 $\times$ 20 pixels) rectangular region in the middle of the GV. Data from two different oocytes is shown. For the first oocyte, the lack of entry of cyclin B-GFP in the first several minutes is seen. Cyclin B-GFP begins to enter at ~7–8 min, and 70-kDa dextran entry begins a few minutes after cyclin B-GFP. Imaging of the second oocyte was begun at a later time, so that the initial lack of entry of cyclin B-GFP is not as clearly documented. The data from this oocyte is shown because nuclear envelope breakdown occurred at a time closer to that of uninjected controls (see RESULTS). The time when GVBD occurred is indicated on the two graphs by "+" symbols. (C) Image sequence for the oocyte shown in B. The oocyte was oriented so that the animal vegetal axis was in the plane of focus of the microscope. The GV is positioned close to the cell surface at the animal pole, and the centrosomes are present in the small region between the GV and the cell surface (Otto and Schroeder, 1984). Cyclin B-GFP enters from the side of the nucleus closest to the centrosomes. Cyclin B-GFP fluorescence seems to accumulate in the centrosomal region, and breakdown of the membrane permeability barrier as monitored by the 70-kDa dextran also occurs at the animal pole side of the nucleus. "cbdex.mov" is a movie of this image sequence. Bar, 50 μm.

REFERENCES

Beckhelling, C., Chang, P., Chevalier, S., Ford, C., and Houliston, E. 2003. Pre-MPF associates with annulate lamellae in *Xenopus* oocytes and egg extracts. Mol. Biol. Cell *14*, 1125–1137.

Beckhelling, C., Perez-Mongiovi, D., and Houliston, E. (2000). Localised MPF regulation in eggs. Biol. Cell *92*, 245–253.

Borgne, A., Ostvold, A.C., Flament, S., and Meijer, L. (1999). Intra-M phase-promoting factor phosphorylation of cyclin B at the prophase/metaphase transition. J. Biol. Chem. *274*, 11977–11986.

Favreau, C., Worman, H.J., Wozniak, R.W., Frappier, T., and Courvalin, J.-C. (1996). Cell cycle-dependent phosphorylation of nucleoporins and nuclear pore membrane protein Gp210. Biochemistry *35*, 8035–8044.

Hagting, A., Karlsson, C., Clute, P., Jackman, M., and Pines, J. (1998). MPF localization is controlled by nuclear export. EMBO J. *17*, 4127–4138.

Hagting, A., Jackman, M., Simpson, K., and Pines, J. (1999). Translocation of cyclin B1 to the nucleus at prophase requires a phosphorylation-dependent nuclear import signal. Curr. Biol. *9*, 680–689.

Heim, R., Cubitt, A.B., and Tsien, R.Y. (1995). Improved green fluorescence. Nature *373*, 663–664.

Hiramoto, Y. (1962). Microinjection of live spermatozoa into sea urchin eggs. Exp. Cell Res. *27*, 416–426.

Huang, J., and Raff, J.W. (1999). The disappearance of cyclin B at the end of mitosis is regulated spatially in *Drosophila* cells. EMBO J. *18*, 2184–2195.

Jackman, M., Lindon, C., Nigg, E.A., and Pines, J. (2003). Active cyclin B1-Cdk1 first appears on centrosomes in prophase. Nat. Cell Biol. *5*, 143–148.

Jaffe, L.A., Gallo, C.J., Lee, R.H., Ho, Y.-K., and Jones, T.L.Z. (1993). Oocyte maturation in starfish is mediated by the $\beta\gamma$-subunit complex of a G-protein. J. Cell Biol. *121*, 775–783.

Jessus, C., and Beach, D. (1992). Oscillation of MPF is accompanied by periodic association between cdc25 and cdc2-cyclin B. Cell *68*, 323–32.

Kiehart, D.P. (1982). Microinjection of echinoderm eggs: apparatus and procedures. Methods Cell Biol. *25*, 13–31.

Kishimoto, T. (1999). Activation of MPF at meiosis reinitiation in starfish oocytes. Dev. Biol. *214*, 1–8.

Laemmli, U.K. (1970). Cleavage of structural proteins during the assembly of the head of bacteriophage T4. Nature *227*, 680–685.

Lee, T.H., and Kirschner, M.W. (1996). An inhibitor of p34Cdc2/cyclin B that regulates the G2/M transition in *Xenopus* extracts. Proc. Natl. Acad. Sci. USA *93*, 352–356.

Lénárt, P. Rabut, G., Daigle, N., Hand, A.R., Terasaki, M., and Ellenberg, J. (2003). Nuclear envelope breakdown in starfish oocytes proceeds by partial NPC disassembly followed by a rapidly spreading fenestration of nuclear membranes. J. Cell Biol. *160*, 1055–1068.

Lew, D.J., and Kornbluth, S. (1996). Regulatory roles of cyclin dependent kinase phosphorylation in cell cycle control. Curr. Opin. Cell Biol. *8*, 795–804.

Li, J., Meyer, A.N., and Donoghue, D.J. (1997). Nuclear localization of cyclin B1 mediates its biological activity and is regulated by phosphorylation. Proc. Natl. Acad. Sci. USA *94*, 502–507.

Macaulay, C., Meier, E., and Forbes, D.J. (1995). Differential mitotic phosphorylation of proteins of the nuclear pore complex. J. Biol. Chem. *270*, 254–262.

Meijer, L., Borgne, A., Mulner, O., Chong, J.P.J., Blow, J.J., Inagaki, N., Inagaki, M., Delcros, J.G., and Moulinoux, J.P. (1997). Biochemical and cellular effects of roscovitine, a potent and selective inhibitor of the cyclin-dependent kinases cdc2, cdk2 and cdk5. Eur. J. Biochem. *243*, 527–536.

Nurse, P. (1990). Universal control mechanism regulating onset of M-phase. Nature *344*, 503–508.

Okumura, E., Sekiai, T., Hisanaga, S.-I., Tachibana, K., and Kishimoto, T. (1996). Initial triggering of M-phase in starfish oocytes: a possible novel component of maturation-promotoing factor besides Cdc2 kinase. J. Cell Biol. *132*, 125–135.

Okumura, E., Fukuhara, T., Yoshida, H., Hanada, S.-I., Kozutsumi, R., Mori, M., Tachibana, K., and Kishimoto, T. (2002). Akt inhibits Myt1 in the signalling pathway leading to the meiotic G2/M phase transition. Nat. Cell Biol. *4*, 111–116.

Ookata, K., Hisanaga, S.-I., Okano, T., Tachibana, K., and Kishimoto, T. (1992). Relocation and distinct subcellular localization of p34Cdc2-cyclin B complex at meiosis reinitiation in starfish oocytes. EMBO J. *11*, 1763–1772.

Otto, J.J., and Schroeder, T.E. (1984). Microtubule arrays in the cortex and near the germinal vesicle of immature starfish oocytes. Dev. Biol. *101*, 274–281.

Perez-Mongiovi, D., Chang, P., and Houliston, E. (1998). A propagated wave of MPF activation accompanies surface contraction waves at first mitosis in *Xenopus*. J. Cell Sci. *111*, 385–393.

Perez-Mongiovi, D., Beckhelling, C., Chang, P., Ford, C.C., and Houliston, E. (2000). Nuclei and microtubule asters stimulate maturation/M phase promoting factor (MPF) activation in *Xenopus* eggs and egg cytoplasmic extracts. J. Cell Biol. *150*, 963–974.

Peter, M., Le Peuch, C., Labbe, C., Meyer, A.N., Donoghue, D.J., and Doree, M. (2002). Initial activation of cyclin-B1-cdc kinase requires phosphorylation of cyclin B1. EMBO Rep. *3*, 551–556.

Peters, R. (1984). Nucleo-cytoplasmic flux and intracellular mobility in single hepatocytes measured by fluorescence microphotolysis. EMBO J. *3*, 1831–1836.

Picard, A., and Peaucellier, G. (1998). Behavior of cyclin B and cyclin B-dependent kinase during starfish oocyte meiosis reinitiation: evidence for non-identity with MPF. Biol Cell. *90*, 487–496.

Pines, J. (1999). Checkpoint on the nuclear frontier. Nature *397*, 104–105.

Pines, J., and Hunter, T. (1991). Human cyclins A and B1 are differentially located in the cell and undergo cell cycle-dependent nuclear transport. J. Cell Biol. *115*, 1–17.

Rankin, S., and Kirschner, M.W. (1997). The surface contraction waves of *Xenopus* eggs reflect the metachronous cell-cycle state of the cytoplasm. Curr. Biol. *7*, 451–454.

Tachibana, K., Ishiura, M., Uchida, T., and Kishimoto, T. (1990). The starfish egg mRNA responsible for meiosis reinitiation encodes cyclin. Dev. Biol. *140*, 241–252.

Takizawa, C.G., and Morgan, D.O. (2000). Control of mitosis by changes in the subcellular location of cyclin-B1-Cdk1 and Cdc25C. Curr. Opin. Cell Biol. *12*, 658–665.

Tang, T.L., Freeman, R.M., O'Reilly, A.M., Neel, B.G., and Sokol., S.Y. (1995). The SH2-containing protein-tyrosine phosphatase SH-PTP2 is required upstream of MPA kinase for early *Xenopus* development. Cell *80*, 473–483.

Tao-Cheng, J.H., Vinade, L., Pozzo-Miller, L.D., Reese, T.S., and Dosemeci, A. (2002). Calcium/calmodulin-dependent protein kinase II clusters in adult rat hippocampal slices. Neuroscience *115*, 435–440.

Terasaki, M. (1994). Redistribution of cytoplasmic components during germinal vesicle breakdown in starfish oocytes. J. Cell Sci. *107*, 1797–1805.

Terasaki, M. (2000). Dynamics of the ER and Golgi apparatus during early sea urchin development. Mol. Biol. Cell *11*, 897–914.

Terasaki, M., Campagnola, P., Rolls, M.M., Stein, P., Ellenberg, J., Hinkle, B., and Slepchenko, B. (2001). A new model for nuclear envelope breakdown. Mol. Biol. Cell *12*, 503–510.

Terasaki, M., Jaffe, L.A., Hunnicutt, G.R., and Hammer, III, J.A. (1996). Structural change of the endoplasmic reticulum during fertilization: evidence for loss of membrane continuity using the green fluorescent protein. Dev. Biol. *179*, 320–328.

Toyoshima, F., Moriguchi, T., Wada, A., Fukuda, M., and Nishida, E. (1998). Nuclear export of cyclin B1 and its possible role in the DNA damage-induced G2 checkpoint. EMBO J. *17*, 2728–2735.

Westendorf, J.M., Swenson, K.I., and Ruderman, J.V. (1989). The role of cyclin B in meiosis I. J. Cell Biol. *108*, 1431–1444.

Yang, J., Bardes, E.S.G., Moore, J.D., Brennan, J., Powers, M.A., and Kornbluth, S. (1998). Control of cyclin B1 localization through regulated binding of the nuclear export factor CRM1. Genes Dev. *12*, 2131–2143.

Zheng, X.F., and Ruderman, J.V. (1993). Functional analysis of the P box, a domain in cyclin B required for the activation of Cdc25. Cell *75*, 155–164.